

Factors controlling the microstructure of $\text{Ce}_{0.9}\text{Gd}_{0.1}\text{O}_{2-\delta}$ films in pulsed laser deposition process

K. RODRIGO, S. HEIROTH^a, M. DÖBELT^b, N. PRYDS^{*}, S. LINDEROTH, J. SCHOU^c, T. LIPPERT^a

Fuel Cells and Solid State Chemistry Division, Risø DTU, Technical University of Denmark, DK-4000 Roskilde, Denmark

^aPaul Scherrer Institut, General Energy Research Department, CH-5232 Villigen PSI, Switzerland

^bIon Beam Physics, Paul Scherrer Institute and ETH Zurich, 8093 Zurich, Switzerland

^cDepartment of Photonics Engineering, Risø Campus, Technical University of Denmark, DK-4000 Roskilde, Denmark

Films of $\text{Ce}_{0.9}\text{Gd}_{0.1}\text{O}_{2-\delta}$ (CGO10) are prepared at a range of conditions by pulsed laser deposition (PLD) on a single crystal Si (100) and MgO (100), and on a polycrystalline Pt/MgO (100) substrate. The relationship between the film microstructure, crystallography, chemical composition and PLD processing parameters is studied. It is found that the laser fluence has no significant impact on the film density, whereas the substrate temperature and the oxygen pressure are of essential importance for the film microstructure development. The reduction of deposition temperature, down to 250 °C, together with a lowered oxygen pressure of 0.05 mbar, significantly inhibits the growth of columnar structures. Further decrease in oxygen pressure, to 0.005 mbar, promotes films densification, but a stress build-up is observed and leads to a lattice-parameter enlargement of the coatings. The chemical films composition is affected by the applied fluence. At a low fluence, 0.5 J/cm², a congruent transfer is obtained while a relative Gd enrichment results for substantially higher fluences (3.5-5.5 J/cm²).

(Received June 22, 2009; accepted November 17, 2009)

Keywords: Gadolinia-doped ceria, Pulsed laser deposition, Low temperature deposition, Stress

1. Introduction

Ceria-based materials attract a great deal of attention due to their applications as gas separation membranes [1], catalysts [2-3] or electrolyte materials for solid oxide fuel cells (SOFCs) [4-6]. Ceria, doped with 10 mol% gadolinia (CGO10), is of particular interest for SOFCs operating at reduced temperature due to higher ionic conductivity compared to the conventional yttria stabilized zirconia (YSZ). Moreover, recently emerging application areas (e.g. batteries in portable electronics) have resulted in novel variants of SOFCs, namely micro-SOFCs [7-8]. These new technologies make the development of electrolyte materials in the form of heteroepitaxial coatings important. Thin films can be readily prepared using pulsed laser deposition (PLD), a technique known for its versatility with a variety of deposited materials [9]. However, the microstructure of coatings prepared by PLD is often columnar and porous. For an SOFC electrolyte working in a traditional arrangement, dense and crack-free films are essential, such that the fuel and combustion gas are separated to ensure electrical and gas tightness. In a physical vapour deposition (PVD) process such as PLD, the films density and microstructure is governed by two major factors: (i) the degree of atom-atom and atom-surface interactions; and (ii) the energy delivered to the system by substrate heating or the energy carried by the species impinging onto the substrate [10]. Studies on the relationship between the film microstructure and the substrate temperature led to the development of structural

zone models (SZMs) [11-13] for coatings prepared by the PVD processes of thermal evaporation and magnetron sputtering. Recently, similar models [14] were reported for coatings prepared by PLD. Furthermore, the relationship between the kinetic energy of the ablated species and the film density in PLD was expressed in an analytical model [15-17]. This model correlated the kinetic energy of the atoms with the laser fluence, pressure of background gas and the substrate-to-target distance. Unfortunately energetic atoms or ions impinging onto the growing film often introduce undesired defects in the film structure that are manifested as an intrinsic stress [18-19]. In films prepared on foreign substrates, mismatch of the lattice parameter and the thermal expansion coefficient (TEC) between coating and the substrate leads to additional sources of intrinsic and extrinsic stress components. Stress related phenomena in PLD-prepared CGO10 films were not considered until now. However, stress-induced failure has already been recognised for YSZ and CGO membranes prepared by magnetron sputtering and e-beam evaporation [20].

This study is focused on two aspects of thin CGO10 electrolyte film deposition: (i) film densification and (ii) stress induced in the coatings, as indicated by the deviation of the film lattice constant from the bulk value. We investigate the relation between the deposition temperature, oxygen pressure in PLD chamber, the resulting microstructure and residual stresses in the CGO10 coatings. In particular, we consider the low temperature deposition due to its advantages in reducing

both the TEC mismatch and inter-diffusion of materials which could negatively affect the electrolyte operation.

2. Experimental procedure

A ceramic target for PLD was prepared from CGO10 powder (Rhodia). The CGO10 powder was mixed with 4 wt% PVA binder and dried in a laboratory beaker. The dried powder was subsequently crushed in an agate mortar and sieved. Pellets were pressed in an uniaxial press (2 ton for 1 min) and isostatic press (60 ton for 0.5 min). The pellets were sintered according to the following procedure: heating to 450 °C with a rate of 15 °C/h; heating from 450 °C to 1500 °C with a rate of 50 °C/h; sintering at 1500 °C for 12 h and cooling to room temperature with a rate of 50 °C/h. The phase purity of the target was confirmed by X-ray diffraction (XRD).

Thin films were prepared by PLD technique in a vacuum chamber with a base pressure of 10^{-6} mbar. An excimer laser beam at a wavelength of 248 nm, pulse length of 20 ns, 330 mJ direct output energy and 40 Hz repetition rate was focused on a rotating target. By varying the focusing optics we obtained the following laser fluence on the target: 0.5 J/cm², 3.5 J/cm² and 5.5 J/cm². The oxygen background gas pressure was varied from 0.1 to 0.005 mbar. The laser-ejected material was collected on substrates placed at a distance of ~65 mm from the target. The substrates used in the experiments were single crystal Si (100) and MgO (100), and polycrystalline porous Pt grown by sputtering deposition onto MgO (100). All substrates were cleaned in ethanol prior to depositions. No effort was made to remove the native SiO₂ growing on the Si. The temperature of the substrates was varied from 25 °C to 750 °C. All films were deposited for 15 min leading to the coating thickness ranging from about 1 µm, for films prepared at 0.1 mbar O₂, to about 400 nm, for coatings made at 0.005 mbar O₂.

The thickness and structure of the nanocrystalline films were analyzed by a high resolution scanning electron microscope (Zeiss Supra) equipped with a field emission gun. Micrographs of top structures and cross-sections of the films were obtained by secondary electron detector (SE2) as well as by an inlens detector. The micrographs were obtained with an acceleration voltage of 1 - 5 kV, 2 - 3 mm working distance and 7.5 - 10 µm apertures.

Crystallographic phase and film orientation were obtained by X-ray diffraction (XRD) using a STOE STADIP diffractometer with Cu K_α radiation, equipped with a Ge (111) monochromator eliminating the CuK_{α2} line. Typically $\theta - 2\theta$ XRD scans were obtained in the range of 20 - 90 deg with resolution of 0.02 deg/step and 17 s time window per each step. The position of diffraction lines was estimated using single line analysis with pseudo-Voigt line-shape by Topas3 software [21]. The Si (400) and MgO (200) reflections from the substrate served as internal standards. Details regarding the substrate properties are collected in Table 1. Selected samples were also analyzed on a Bruker D8 diffractometer with CuK_α radiation to confirm the observed dependencies. The lattice constant for each diffraction line was calculated from the Bragg's equation applied to the CGO10 cubic system.

The chemical composition of the CGO films was investigated by Rutherford backscattering spectrometry (RBS) at the ion beam analytics facilities at ETH Zürich using either 2 MeV or 5 MeV ⁴He ions as projectiles from the Van de Graaf accelerator. RUMP software [30] was utilized to analyze the data. From the 2 MeV spectrum, the (Ce, Gd):O ratio could be obtained. The 5 MeV spectrum allows a determination of the Ce:Gd stoichiometry due to an enhanced resolution in the high Z region. The RBS results were confirmed by Elastic Recoil Detection Analysis (ERDA) using 12 MeV ¹²⁷I projectiles at glancing incidence. The recoiling target atoms were detected by a TOF spectrometer combined with a gas ionization chamber.

3. Results and discussion

Guided by the model outlined by Gottmann et al. [15-17], the impact of laser fluence and oxygen pressure on the film microstructure was inspected while keeping the substrate-to-target distance constant. Films prepared at a fluence of 0.5, 3.5 and 5.5 J/cm², and with an oxygen pressure of 0.1 mbar display similarities in the microstructure, independent of the substrate temperature. Typical coatings (Fig. 1) gradually change from porous agglomerates of thin needle-like columns characteristic to room temperature depositions (Fig.1 a) to mainly columnar formations, 20 - 50 nm wide, at elevated temperatures (Fig. 1 b - d). The density of this type of coatings can reach 85-90 % of the bulk value, as derived from SEM micrographs (data not shown here).

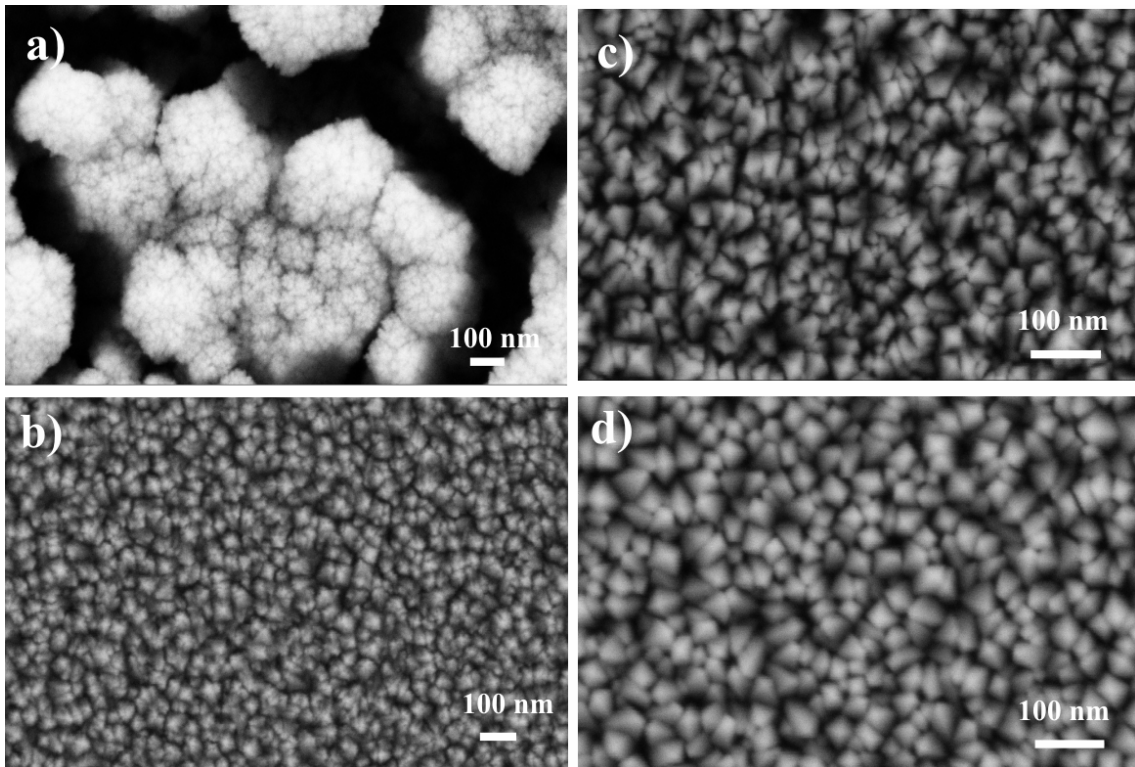


Fig. 1. Top view SEM micrographs of CGO10 films prepared on Si (100). Each film was deposited for 15 min at laser fluence of 5.5 J/cm^2 , 40 Hz pulse repetition rate, 0.1 mbar O_2 pressure, and temperature of a) 25°C , b) 250°C , c) 500°C , and d) 750°C . All micrographs were obtained by SE2 detector.

It appears that the applied oxygen pressure counteracts any effect of the increased fluence on the kinetic energy of the ablated atoms such that no improvement in film densification is seen. Additional heating of the substrate has no significant influence on the film microstructure (Fig. 1 c, d) indicating clearly that the low rate of collisions between background gas and ablated species is the main factor to be considered for film densification. This is supported by Fig. 2, which depicts results for films prepared at a laser fluence as low as 0.5 J/cm^2 . A noticeable change in film microstructure is observed when the oxygen pressure is reduced. At low pressure the average energy of the plume species is higher, and more energy is transferred to the growing film by high-energy plume atoms, which leads to compact films (Fig. 2 b, c, e, f). In fact, Coccia et al. [31] reported that a significant flux of Ce^+ ions with kinetic energies in a range of 20 - 150 eV in high vacuum and at a fluence of 1.67 J/cm^2 is present in the plume ablated from the CGO10 target. Although our depositions are performed in the presence of a background gas and at a lower fluence, the change from porous to compact layers is apparent and is most likely caused by the arrival of energetic species. The reduction of deposition temperature, together with low oxygen pressure, almost entirely inhibits the development of columnar structures (Fig. 2 b, c), while columnar or grain-like features are always observed in coatings

prepared at 750°C (Fig. 2 e, f). Note that the low deposition temperature might reduce the thermal migration of the atoms on the surface. This, combined with a low energy input from the ablated atoms, at high oxygen pressure, inhibits the nucleation and coalescence. Atoms arriving on the surface are virtually immobilised and, before being rearranged, they are buried by the next generations of species supplied to the surface. This so-called “ballistic” deposition results in the film structures in the form of voided columns (Fig. 1 a and 2 a). At higher deposition temperature (Fig. 2 d) the growth is thermally activated. Atoms arriving on the surface acquire more energy from the environment and the growth might be governed by atom diffusion on the film surface. Formation of columnar structures is driven by surface energy minimization. When the pressure is reduced even further, the energy of species arriving on the film surface increases as discussed above. This leads to an energy-enhanced deposition process where film densification is achieved by forward scattering of the film atoms into voids in the coating, as seen in the films prepared at 250°C (Fig. 2 b, c). Coatings prepared at 750°C and at low oxygen pressure (Fig. 2 e, f), although appearing compact, still form columnar grains. The lack of bulk diffusion of the atoms delivered to the growing film is probably the main factor determining the microstructure at these conditions.

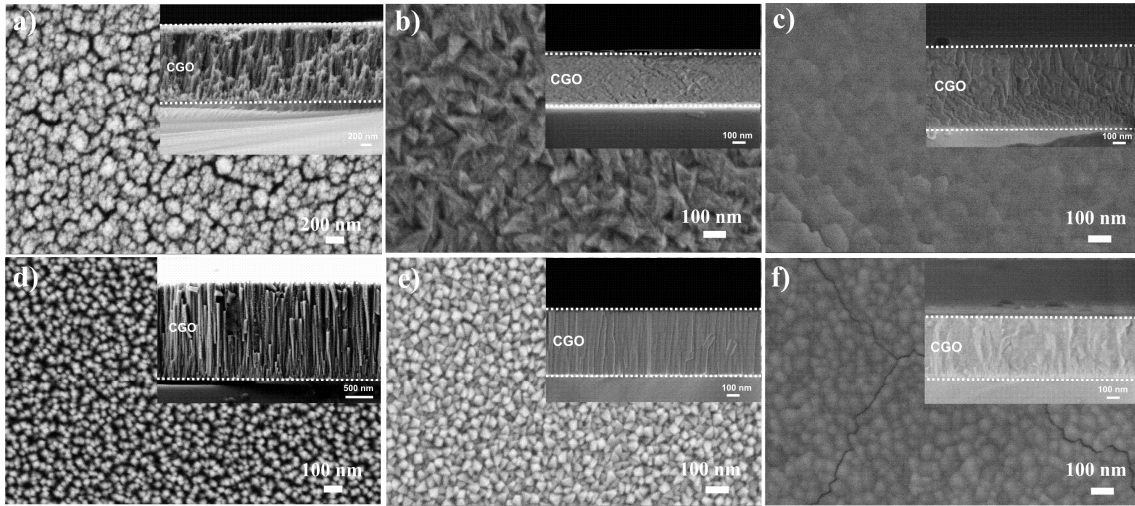


Fig. 2. Top view SEM micrographs of CGO10 films deposited on Si (100). Insets present cross-sections of the coatings. Films were deposited at laser fluence of 0.5 J/cm^2 , 40 Hz pulse repetition rate, varying O_2 pressure: first column 0.1 mbar O_2 , second column 0.05 mbar O_2 , third column 0.005 mbar O_2 , and temperature: a-c) 250 °C, e-f) 750 °C. Insets in a, d) were obtained by SE2 detector, remaining micrographs obtained by inlens detector. Insets in a) and d) present cross-sections of films deposited for 1 h.

No stress-related damage is observed in the coatings, except for the film prepared at 750 °C and 0.005 mbar, where crack formation is clearly visible (Fig. 2 f). In this case, the significance of the thermal component (see Table 1 for details) of the residual stress has to be higher than the intrinsic part, i.e. related to any imperfection of crystal lattice, since a relaxation of the latter is expected due to promoted self-diffusion of atoms at this temperature. Stress-release by atom diffusion seems unlikely in films prepared at 250 °C indicating that the film damage due to the TEC mismatch might be dominant in this case. However, no damage is observed in films prepared on Si (Fig. 2 b, c) that has the least TEC compatibility with CGO10 (see Table 1 for details).

Table 1. Properties of the bulk CGO10 and the substrates used in the experiments.

Material	Lattice parameter	Lattice mismatch	TEC* [10^{-6} K^{-1}]	
	a [Å]	f [%]	250 °C	750 °C
CGO10	5.418 [22]	-	10.5	11 [26]
Si	5.431 [23]	0.2	3.5	4.2 [27]
MgO	4.211 [24]	29	12.7	15.0[28]
Pt	3.923 [25]	38	9.5	10.8[29]

*approximate values; $f = |(a_{\text{CGO10}} - a_{\text{substrate}}) / a_{\text{substrate}}| 100\%$

The microstructure of the prepared films has its analog in XRD spectra (Fig 3). Polycrystalline films with cubic fluorite structure characteristic to bulk CGO10 were prepared. Highly textured films are produced at 750 °C, independent of the applied oxygen pressure (Fig. 3 a). The {111}-texture, which was observed at 0.05 mbar and 0.005 mbar, represents the facet with the lowest surface energy for the fluorite type of crystallographic structures [32], demonstrating thermodynamically driven growth. On the contrary, at 0.1 mbar the high pressure of oxygen during film growth, leads probably to kinetically driven growth, where the growth rate on the {200} facet is higher than on any other facet. The crystallinity of films produced at 250 °C varies with the applied oxygen pressure (Fig. 3 b). The poorly developed crystallographic phase of coatings prepared at 0.1 mbar of oxygen is probably a result of the low atom mobility at this condition. Low oxygen pressure, 0.05 mbar, promotes the {111} texture, whereas depositions at 0.005 mbar lead to the {311} as the preferred orientation.

More importantly, the low deposition temperature and the high energy of the ablated ions arriving on the growing film, at 0.005 mbar O_2 , result in significant change in the position of Bragg reflections, indicating a lattice constant deviation from the bulk value (inset in Fig. 3 b). This phenomenon is clearly observed in Fig. 4, where values of apparent lattice parameters a_{hkl} are plotted against $\cos\theta\cot\theta$ - an extrapolation function minimizing systematic errors in XRD experiments [33]. This approach makes it possible to determine the lattice parameter a_o in a cubic system without the need of an internal standard [34] (inset in Fig. 4 a).

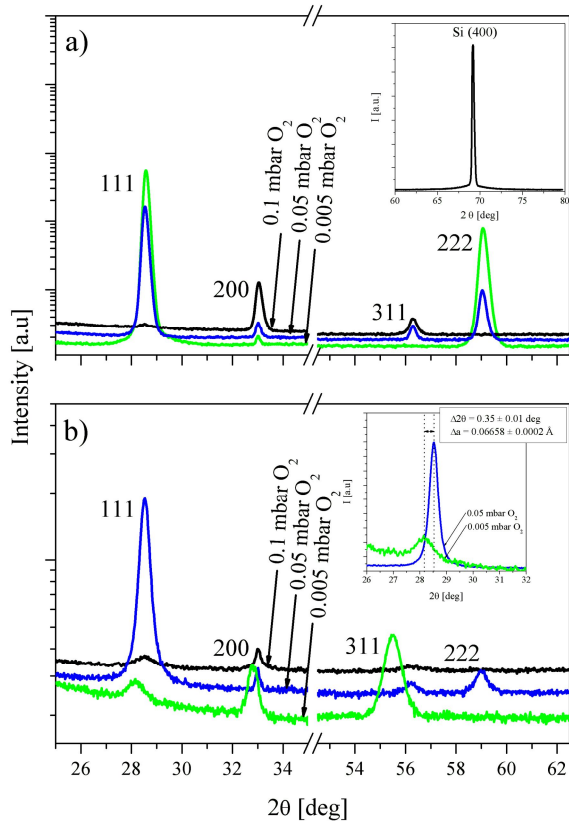


Fig.3. θ - 2θ XRD spectra of CGO10 films deposited on Si (100). Each film was deposited for 15 min at laser fluence of 0.5 J/cm^2 , 40 Hz pulse repetition rate, temperature of a) $750 \text{ }^\circ\text{C}$, b) $250 \text{ }^\circ\text{C}$ and varying oxygen background pressure (indicated in the graph). Main reflections of CGO fluorite structure are indicated in the graph. Reflection from the Si (100) substrate is indicated in the inset in a, whereas inset in b presents the difference in (111) peak position for samples prepared at 0.05 mbar and 0.005 mbar O_2 .

However, when this approach is applied to thin films, it results in significant scattering or offset of a_{hkl} values [34-36], what is understood as a manifestation of hkl dependent residual stress of various origin. As seen in Fig. 4, values of a_{hkl} , except from departing from linear dependence, are assembling around two distinct a values, i.e. 5.42 \AA and 5.48 \AA (about 1% difference). An increased level of a_{hkl} is observed in films prepared at low temperature and reduced oxygen pressure down to 0.005 mbar (Fig. 4). A weak dependence between the value of a_{hkl} and the substrate type is also seen in Fig. 4. This fact cannot be explained alone by the lattice and the TEC mismatch between coatings and substrates (see Table 1 for details), since this phenomenon is not observed in films prepared at higher oxygen pressure (Fig. 4 b). It is most likely an effect of strains in the film originating from imperfect crystallographic lattice. Film irradiation by highly energetic species combined with low atom mobility, as in the case of low temperature depositions are

likely to result in a lattice with defects. One has to notice, that no influence of the gas pressure on the a_{hkl} in the film prepared at $750 \text{ }^\circ\text{C}$ and 0.005 mbar of oxygen is observed. In this case, the influence of surface diffusion of atoms together with observed film cracking (Fig. 2 f), and probably in-situ annealing of plume-induced defects, are likely to be responsible for the release of residual stress.

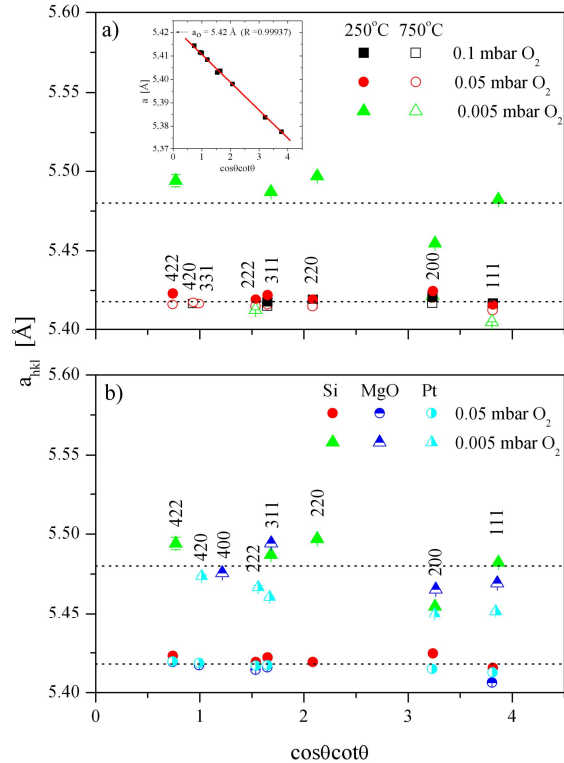


Fig. 4. Apparent lattice parameters a_{hkl} of CGO10 films prepared on a) Si (100) at various deposition temperature and oxygen pressure (details indicated in the graph). b) Comparison of a_{hkl} of CGO10 films prepared on Si (100), MgO (100) and Pt/MgO (100) at $250 \text{ }^\circ\text{C}$ and varying oxygen pressure (indicated in the graph). Inset in a) presents a method of estimation of lattice parameter from a_{hkl} for powder sample of CGO10. The value of lattice parameter obtained by this method is shown in the plot. Miller indexes hkl related to each a_{hkl} are indicated in the graphs.

The importance of crystallographic flaws built into the film during irradiation by highly energetic species was reported previously [19]. Plume-induced stress in CeO_2 films prepared at 0.07 mbar O_2 and at $100 \text{ }^\circ\text{C}$, resulted in a 1.6 % lattice constant distortion. In this case oxygen pressure as high as 0.5 mbar led to deposition of coatings with lattice constants similar to the bulk ceria. Moreover, analogous to our observation, the report indicates that a high deposition temperature does not introduce significant changes in the film lattice constants.

Table 2. Results of RBS analysis for chosen samples.

Temp [°C]	pO ₂ [mbar]	Fluence [J/cm ²]	x(Ce)	x(Gd)	x(O)
750	0.1	0.5	0.9	0.1	1.95
750	0.1	3.5	0.88	0.12	2.0
750	0.1	5.5	0.885	0.115	1.95
250	0.1	0.5	0.91	0.09	*
250	0.05	0.5	0.9	0.1	1.97
250	0.005	0.5	0.91	0.09	1.93

*: not determinable (signal obscured supposedly by sparking of the specimen)

One has to also keep in mind that mechanical stress is interrelated with chemical properties of the sample either in a bulk [37-38] or thin-film form [39]. The lattice expansion in ceria can be associated with oxygen deficiency and thus reduction of ceria from Ce⁺⁴ to Ce⁺³. Assuming that the 1% lattice distortion, observed in our case, relates purely to the increased number of oxygen vacancies in the sample, then the level of reduced ceria yields 15 mol% - a calculation based on Kim's formula [40] for lattice constants of ceria doped with 10 mol% of gadolinia and x mol% of reduced ceria, with Shannon ionic radii [41] used for the estimation. This level of Ce⁺³ would result in oxygen content as low as 1.875 at % instead of 1.95 at % for Ce⁺⁴ based film of CGO10.

To investigate whether chemical stress consist a major contribution to the observed overall stress, the chemical composition of the CGO films was analyzed by ion beam techniques. Fig. 5 shows a representative set of RBS spectra acquired at different projectile energy to derive a) the (Ce+Gd):O respectively b) the Ce:Gd elemental ratio. All spectra reveal a uniform elemental distribution in depth, i. e. no compositional gradient was found. As can be seen from Table 2, which summarizes the quantitative RBS results, the CGO films exhibit a normalized oxygen stoichiometry factor matching the expected value of 1.95 ± 0.05 for the target composition within the experimental accuracy. Regarding the relatively large experimental error, a slight oxygen deficiency cannot be ruled out eventually. However we may note that, if present at all, this effect would be small. The chemical contribution is unlikely to account for the large stress evidenced by XRD for the CGO film deposited at 250°C and low oxygen pressure, in particular since the RBS spectra do not reveal major differences in the oxygen content among the set of samples. The chemical films composition can be however affected by the applied fluence. At a low fluence, 0.5 J/cm², a congruent transfer of material is obtained, while a relative Gd enrichment is observed when substantially higher fluences are applied (3.5 J/cm² – 5.5 J/cm²) (see Table 2 for details).

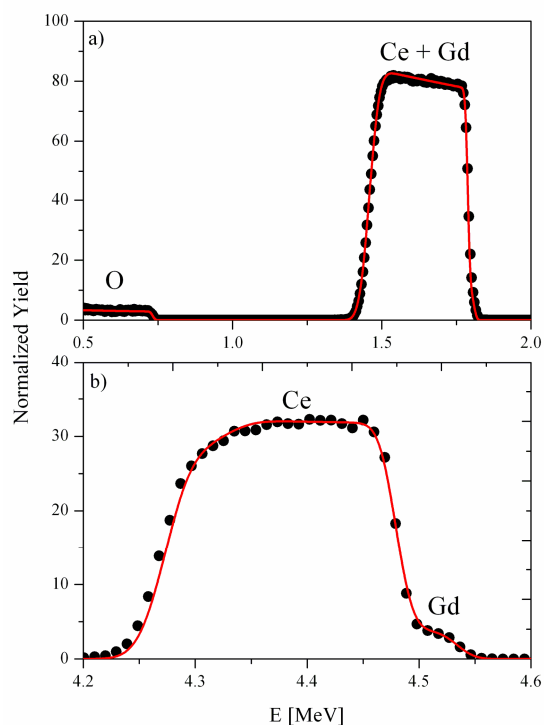


Fig. 5. RBS analysis of the film prepared at 250 °C and 0.05 mbar O₂ using a) 2MeV and b) 5MeV ⁴He ions as projectiles. The spectra have been corrected for contributions of the substrate. Points represent experimental data, while red solid line is obtained from simulation. Estimation of cation composition is within ± 0.005 at%, whereas estimation of oxygen stoichiometry is within ± 0.05 at%.

4. Conclusions

Films of CGO10 were prepared by PLD at a variety of deposition conditions on various substrates ranging from a single crystal Si (100) and MgO (100) to polycrystalline Pt sputtered on Mg (100). We found that low temperature deposition (250 °C) and reduced oxygen pressure (0.05 mbar) during film growth inhibit development of columnar grains. It was also found that further reduction of the oxygen level, down to 0.005 mbar results in compact films, but the a_{hkl} vs. $\cos\theta\cot\theta$ dependence indicates stress-related enlargement of the lattice parameter of the coatings. Variation of a_{hkl} of the films prepared at reduced oxygen pressures, weakly depends on the substrate type indicating that the distortion of the lattice constant might be mainly originating from the increased level of built-in crystallographic defects, an effect related purely to the deposition process. Film irradiation by highly energetic species from the plume of ablated material may also lead to oxygen depletion in the coatings, and, as a result, to the development of chemically induced stress. This source of stress cannot be entirely ruled out. Further investigation has to be undertaken in order to fully clarify the origin of the observed dependencies.

Acknowledgements

The authors would like to thank S. Ohmar and M. Lundberg for valuable discussions and acknowledge the competent technical assistance from Finn Saxild.

References

- [1] Y. Li, J.A. Kliner, M.F. Carolan, J. Eur. Ceram. Soc., **24**, 3613 (2004).
- [2] P. Bera, M. S. Hegde, Catal. Lett., **79**, 75 (2002).
- [3] R. X. Valenzuela, G. Bueno, A. Solbes, F. Sapina, E. Martinez, V. C. Corberan, Topics Catal. **15**, 181 (2001).
- [4] J. A. Kilner, Solid State Ionics, **129**, 13 (2000).
- [5] M. Mogensen, N. M. Sammes, G. A. Topset, Solid State Ionics, **129**, 63 (2000).
- [6] B.C.H. Steele, Solid State Ionics, **129**, 95 (2000).
- [7] H. Huang, M. Nakamura, P. Su, R. Fasching, Y. Saito, F. B. Prinz, J. Electrochem. Soc., **154**, B20 (2007).
- [8] X.Chen, N.J. Wu, L. Smith, A. Ignatiev, Appl. Phys. Lett., **84**, 2700 (2004).
- [9] R. Eason, Pulsed Laser Deposition of Thin Films: Applications-Led Growth of Functional Materials, Wiley, New York, 2007
- [10] D. L. Smith, Thin - Film Deposition, MacGraw - Hill, 1995, p. 215.
- [11] J. A. Thornton, Ann. Rev. Mater. Sci., **7**, 239 (1977).
- [12] B. A. Movchan, A. V. Demchishin, Phys. Met. Metallogr. **28**, 83 (1969).
- [13] I. Petrov, P.B. Barna, L.Hultman, J.E. Greene, J. Vac. Sci. Technol., **A32**, S117 (2003).
- [14] A. Infortuna, A. Harvey, L. Gauckler, Adv. Funct. Mater. **18**(1), 127 (2008).
- [15] J. Gottmann, A. Husmann, T. Klotzbucher, E. W. Kreutz, Surf. Coat. Tech, **100-101**, 415 (1998)
- [16] J. Gottmann, E.W. Kreutz, Surf. Coat. Tech, **116-119**, 1189 (1999).
- [17] E. W. Kreutz, J. Gottmann, M.Mergens, T. Klotzbucher, B. Vosseler, Surf. Coat. Tech, **116-119**, 1219 (1999).
- [18] M. Birkholz, Thin film Analysis by X-Ray Scattering, Wiley-Vch Verlag, Weinheim, 2006, p. 272
- [19] D. P. Norton, C.Park, J.D. Budai, S.J. Pennycook, C. Proteau, Appl. Phys. Lett, **75**(15), 2134 (1999).
- [20] C. D. Baertch, K. F. Jensen, J. L. Hertz, H. Tuller, S. T. Vengallatore, S. M. Spearing, M. A. Schmidt, J. Mater. Res., **19**, 2604 (2004).
- [21] Diffrac^{plus} Topas P 3, Bruker AXS GmbH D-76187 Karlsruhe, Germany (2003).
- [22] G. Brauer, H. Gradinger, Zeitschrift fuer Anorganische und Allgemeine Chemie, **276**, 209 (1954).
- [23] <http://physics.nist.gov/cgi-bin/cuu/Value?asil>
- [24] R. W. G. Wyckoff, Z. Kristallogr. Krist., **62**, 529 (1925).
- [25] C. A. Swanson, J. Tatge., Natl. Bur. Stand. (U.S.), Circ. **539**, 31 (1953).
- [26] H. Hayashi, K. Kanoh, C. J. Quan, H. Inaba, S. Wang, M. Dokiya, H. Tagawa, Solid State Ionics, **132**, 227 (2000).
- [27] V. M. Glazov, A. S. Pashinkin, High Temp., **39**, 413 (2001).
- [28] G. K. White, O. L. Andersen, J. Appl. Phys. **37**, 430 (1966).
- [29] R. K. Kirby, Int. J. Thermophys. **12**, 679 (1991).
- [30] L. R. Doolittle, Nucl. Instrum. Methods Phys. Res., Sect. B, **9**, 344 (1985).
- [31] L. G. Coccia, G. C. Tyrrell, J. A. Kliner, D. Waller, R. J. Chater, I. W. Boyd, Appl. Surf. Sci. **96-98**, 795 (1996).
- [32] D. L. Smith, *op. cit.*, p. 142.
- [33] B. D. Cullity, Elements of X-Ray Diffraction, Addison -Wesley, 1978, p. 356
- [34] H. W. King, E.A. Payzant, Advances in X-Ray Analysis, , Plenum Press, New York, **36**, 663 (1993).
- [35] A. Laor, L. Zevin, J. Pelleg, Thin Solid Films **232**, 143 (1993).
- [36] D. S. Rickerby, A.M. Jones, B. A Bellamy, Surf. Coat. Tech, **37**, 111 (1989).
- [37] A. Atkinson, Solid State Ionics, **95**, 249 (1997).
- [38] A. Atkinson, T. Ramos, Solid State Ionics, **129**, 259 (2000).
- [39] J. P. Nair, E. Wachtel, I. Lubomirsky, J. Fleig, J. Maier, Adv. Mater, **15**, 2077 (2003).
- [40] D. J. Kim, J. Am. Ceram. Soc., **72**, 1415 (1989).
- [41] D. R. Shannon, Acta. Crystallogr. Sect. A, **32**, 751 (1976).

*Corresponding author: nipr@risoe.dtu.dk